JACS
JOURNAL OF THE AMERICAN CHEMICAL SOCIETY

Article

pubs.acs.org/JACS

Multiprotein Heme Shuttle Pathway in *Staphylococcus aureus*: Iron-Regulated Surface Determinant Cog-Wheel Kinetics

Michael T. Tiedemann,[†] David E. Heinrichs,[§] and Martin J. Stillman*,[†]

[†]Department of Chemistry, The University of Western Ontario, London, Ontario, Canada, N6A 5B7

[§]Department of Microbiology and Immunology, The University of Western Ontario, London, Ontario, Canada, N6A 5C1

Supporting Information

ABSTRACT: Iron is a critically important nutrient for all species. Bacteria have evolved specialist survival systems to chelate and transport iron across the wall and membrane into the cytoplasm. One such system in the human pathogenic bacteria *Staphylococcus aureus* involves extracting heme from hemoglobin and then transporting the intact heme across the wall and membrane. The iron-regulated surface determinant (Isd) proteins act in concert to carry out the heme scavenging and subsequent transport. While details of the static heme-binding reaction are currently quite well known, little mechanistic data are available. In this paper, we describe detailed time-resolved mass spectral and magnetic circular dichroism spectral data recorded as heme is transferred unidirectionally from holo-IsdA to apo-IsdE via IsdC. The electrospray mass spectral data simultaneously monitor the concentrations of six protein species involved in the trans-wall transport of the extracted heme and show for the first time the mechanistic details of heme transfer that is key to the *Staphylococcus aureus* Isd heme-scavenging system. Bimolecular kinetic analysis of the ESI-mass spectral data shows that heme transfer from IsdA to IsdC is very fast, whereas the subsequent heme transfer from IsdC to IsdE is slower. Under limiting IsdC conditions, the IsdC intermediary cycles between heme-free and heme-containing forms until either all heme has been transferred from holo-IsdA or no further apo-IsdE is available. The data show that a unique role for IsdC is acting as the central cog-wheel that facilitates heme transfer from IsdA to IsdE.

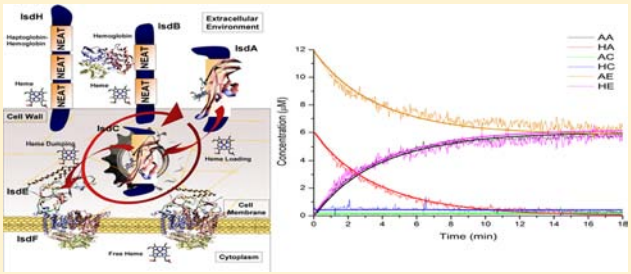

INTRODUCTION

Iron is an essential nutrient to all forms of life, being critical for a range of functions including oxygen transport and energy metabolism. However, free ferric (Fe^{3+}) iron is almost insoluble in aerobic systems, with an estimated concentration of approximately 10^{-18} M.[1,2] Under normal biological conditions iron is sequestered in ferritin, transferrin, and heme proteins in mammals. As a result, bacteria have developed multiple iron acquisition systems to facilitate their survival.[3−6] A readily accessible and the most abundant iron source for bacteria in mammals is iron-protoporphyrin IX (heme), which is typically bound in proteins such as hemoglobin and myoglobin. Bacteria can extract heme from hemoglobin and myoglobin using protein-based extraction pathways that generally isolate and subsequently bind the heme to the amino acid ligands His and Tyr.[7−9] The heme is then transferred through the bacterial cell wall via a series of heme-binding proteins and finally to an ABC heme transporter to cross the membrane into the cytoplasm, where the iron is then extracted from the protoporphyrin IX with heme-degrading proteins. Examples of bacterial heme acquisition systems include the *phu* system in *Pseudomonas aeruginosa*, the *has* system in *Serratia marcescens*, and the *shu* system in *Shigella dysenteriae*.[9] The *isd* system in *Staphylococcus aureus* also carries out this function and is the heme-scavenging protein system that is the focus of this present study.[9]

Antibiotic-resistant bacterial infections by *S. aureus* cause a range of infections and diseases, most significantly life-threatening pneumonia, meningitis, endocarditis, and septicemia.[10,11] The iron-regulated surface determinant (Isd) protein system extracts iron from heme in hemoglobin and myoglobin.[12,13] The *isd* gene cluster was first identified in 2002,[14−16] and in 2003 Mazmanian et al.[17] proposed that the Isd series of proteins acts as a heme-transfer pathway across the cell wall and through the membrane of the Gram-positive *S. aureus*. In *S. aureus* the Isd system consists of nine iron-regulated proteins: IsdA, IsdB, IsdC, and IsdH, which are cell-wall-anchored surface proteins; IsdE and IsdF, which constitute a substrate-binding protein and the membrane-localized ABC transporter; and, finally, IsdG and IsdI, which are heme-degrading enzymes in the cytoplasm.[18−20] Defining the detailed function of the Isd proteins takes on added significance when one considers that several of the Isd proteins have been demonstrated to play a significant role in *S. aureus* pathogenesis, using several different culture and animal models that tested for tissue adherence, colonization, persistence, and ability to cause tissue abscesses.[21−24]

Received: May 25, 2012
Published: September 17, 2012

Considerable research has provided the structures and some mechanistic details of the Isd-mediated heme acquisition systems in *S. aureus*. A number of individual reactions of the Isd protein system have been reported, including the binding of hemoglobin by IsdB,[13,25] the IsdH-dependent binding of haptoglobin and haptoglobin−hemoglobin,[26,27] and heme binding by IsdA, IsdB, IsdC, IsdE, and IsdH.[8,28−31] The proteins IsdA, IsdB, IsdC, and IsdH each contain at least one near transporter (NEAT) domain that adopts a beta sandwich structure to bind one ferric heme into a groove with heme-iron coordination via Tyr.[32,33] IsdE, a lipoprotein and member of the class III substrate-binding proteins, binds heme into a shallow groove between two α/β lobes of the protein, using His and Met to coordinate to the ferric-heme-iron.[34]

Key to the proposal for the role of the Isd series of proteins in iron acquisition in *S. aureus* is that heme passes from protein to protein in such a manner as to move spatially through first the ∼90 nm thick bacterial wall and then the bacterial membrane into the cytoplasm. Experimental evidence for the trans-wall and trans-membrane sections of the mechanism for this channeling process has not been reported to date. Techniques previously used to study the Isd system include UV−visible absorption spectroscopy (heme transfer from IsdA to IsdC), crystallography for protein structure and heme-binding ligands, magnetic circular dichroism (MCD) spectral data to elucidate ligand binding to heme, and electrospray ionization mass spectrometry (ESI-MS) to elucidate the heme-transfer pathway. Individual heme-transfer reactions have been predominantly studied by UV−visible absorption spectroscopy, where the heme-transfer kinetics between pairs of proteins has been analyzed by stopped-flow spectroscopy.[13,25,31,35,36] However, a major difficulty arises when using UV−visible absorption spectroscopy to monitor heme binding when the amino acid residues binding the iron of the heme in both the donor and receiver proteins are similar or the same, which is the case for several proteins within the Isd system. This results in very similar optical spectra, leading to very small ΔA changes in the spectra during heme transfer. Mass spectral data overcome these limitations by readily distinguishing the differing masses of the heme-free apo-proteins from heme-free denatured apo-proteins and from the native heme-bound holo-proteins. ESI-MS has been previously been shown to be a powerful technique in elucidating the mechanism of protein folding or cofactor transfer in systems.[37−41] In previous work, it was also shown that ferric heme transfer occurred in an unusual unidirectional fashion down the pathway of the series of Isd proteins, where we indicate the proximal amino acid residue in parentheses, IsdB (Tyr)→IsdA (Tyr)→IsdC (Tyr)→IsdE (His) or, alternatively, initiating from IsdH, IsdH (Tyr)→IsdA→IsdC→IsdE. Finally it was shown that heme transfer through the cell wall must occur via IsdC, indicating that IsdC acts as the central conduit of the Isd system.[36]

In this paper, the first real-time measurement of heme transfer between the three key proteins in the Isd system involved in the trans-wall channeling are reported. By exploiting the unidirectional nature of the Isd system (that is, heme transfer only takes place from IsdA→IsdC→IsdE) and by using limiting concentrations of IsdC, we have explored the real-time heme-transfer kinetics across these three proteins by MCD spectroscopy and ESI-MS. Time-resolved mass spectral data provide firm evidence for a sequential, multiprotein heme-transfer system. Determining the reaction rates from kinetic measurements for heme transfer between these three Isd proteins provides new information that directly addresses the hypothesis that the proteins function in concert as a heme shuttle system in the Gram-positive bacteria cell wall.

EXPERIMENTAL METHODS

Gene Cloning, Protein Expression, and Mutation Techniques. DNA encoding residues 62−184 of IsdA, residues 28−150 of IsdC, and residues 32−292 of IsdE were PCR amplified from *S. aureus* RN6390 chromosome and cloned into pET28(+) in such a way as to incorporate N-terminal 6X-His tags. DNA-encoded His-tagged protein was digested out of pET28a(+) and cloned into pBAD30[42] before being introduced into *E. coli* RP523, a *hemB* mutant.[43]

E. coli RP523 cells harboring recombinant plasmids were grown at 30 °C in Luria−Bertani broth (LB; Difco) containing ampicillin (100 μg/mL) and L-arabinose (0.2%). After overnight incubation, cells were harvested and resuspended in binding buffer (10 mM sodium phosphate, pH 7.4, 500 mM NaCl, 10 mM imidazole). Cells were then ruptured in a French pressure cell, and cell lysates were subjected to ultracentrifugation at 150000*g* for 1 h to remove insoluble material. Proteins were purified using a 1 mL HisTrap column (GE Healthcare) and an ÄKTA FPLC system with an elution buffer containing 10 mM sodium phosphate, pH 7.4, 500 mM NaCl, 500 mM imidazole. Proteins were then desalted using a 5 mL HiTrap desalting column (GE Healthcare). The 6X-His tags were removed by incubation with thrombin (10 U/mg protein; GE Healthcare) at room temperature for 16 h and run through a HisTrap column for final purification.

Hemin (Sigma) was dissolved in diluted ammonium hydroxide, pH 10. Protein concentrations were estimated using the extinction coefficients at 280 nm of 28.85 mM^{-1} cm^{-1} for Isd-NEAT-A, 38.26 mM^{-1} cm^{-1} for Isd-NEAT-C, and 20.07 mM^{-1} cm^{-1} for IsdE. These values were determined by calibrating the 280 nm protein band by quantifying completely holo-Isd proteins by Fe atomic absorption spectroscopy using an AA240 instrument with SPS 5 auto sampler (Varian, Canada) and by UV−visible absorption spectroscopy using a Cary 500 instrument (Varian, Canada). Each Isd protein binds only one heme; therefore, the amount of iron present corresponds to the amount of heme, which then corresponds to the amount of Isd protein.

ESI-MS Measurements. Protein solutions were concentrated, desalted, and buffer-exchanged from 10 mM phosphate-buffered saline solution (PBS), pH 7.4, to 20 mM ammonium formate, pH 7.4 (a mass spectrometry-compatible buffer), using Millipore Amicon Ultra-4 centrifuge filter units (10 kDa MWCO) with a Beckman CS-6 swinging-bucket centrifuge (3000 rpm for 10 min per run). Once thoroughly buffer exchanged, proteins were used for ESI-MS measurements.

A Bruker micrOTOF II ESI-TOF mass spectrometer (Bruker, Canada) operated in the positive-ion mode was used for all ESI-MS measurements. Samples in 20 mM ammonium formate buffer, pH 7.4, were infused into the spectrometer at a rate of 600 μL h^{-1} using a microliter infusion pump. The instrument was calibrated with an external CsI standard solution. Data were processed using the Bruker DataAnalysis 4.0 program. Parameters: sample range, 500−4000 m/z; rolling average, 2 × 0.5 Hz; end plate offset, −500 V; nebulizer, 2.0 bar; dry gas temperature, 293 K; flow rate, 8.0 L/min; capillary voltage, 4200 V; capillary exit, 180 V; skimmer 1, 22 V; hexapole, 225.0 V; hexapole rf, 600 V. The complete kinetic run was measured from a single mixture.

Heme-Transfer Reactions. To monitor heme transfer between the two NEAT domains (IsdA-N and IsdC-N) and IsdE, apo-IsdC-N (for MCD) or holo-IsdC-N (for ESI-MS) was added to a mixture of holo-IsdA-N and apo-IsdE. Previous reports have shown that there is no heme transfer between holo-IsdA-N and apo-IsdE and that no free heme can be detected, so this mixture is stable.[36] The solution was rapidly mixed and then immediately infused into the mass spectrometer. Data were measured continuously for up to 30 min; however, only the first 20 min of data are shown. The protein concentrations were deduced from the normalized relative abundances summed from the charge states of the apo/holo pairs of the respective

proteins at each time interval. The samples were held at a thermostated temperature of 15 °C during infusion for ESI-MS measurements. Each transfer reaction shown is an average of three separate runs.

Kinetic Analysis. To calculate the concentration of each Isd species, the intensities (counts) of the charge states of each Isd protein were summed and then normalized relative to the apo/holo pair. The charge states used for each Isd protein were as follow: apo/holo-IsdA-N, +8 and +7; apo/holo-IsdC-N, +9 and +8; and apo/holo-IsdE, +13, +12, and +11. The concentration data for each species (holo-IsdA-N, apo-IsdA-N, holo-IsdC-N, apo-IsdC-N, holo-IsdE, and apo-IsdE) at each time interval for the complete kinetic reaction were analyzed using the program Copassi.[44] The reaction scheme used is described below in the Results section. Errors were calculated using the standard deviation for each k calculated from the fit.

MCD Spectral Measurements. MCD spectra were measured using an SM2 5.5 T superconducting magnet (Oxford, UK) attached to a J-810 CD spectrometer (Jasco Inc., Japan) with a range of 500−350 at 2 nm steps with a 1 s response time and no delay between scans. A t_0 spectrum was measured with a solution containing holo-IsdA-N and apo-IsdE with the absence of apo-IsdC-N (conditions under which no heme transfer could take place). Spectra were then measured continuously for 40 min. A t_∞ spectrum was recorded 90 min after the kinetic run had started.

UV−Visible Absorption Spectral Measurements. Continuous UV−visible absorption spectral scans were measured on a Cary50 Bio spectrometer (Varian, Canada) using the Scanning Kinetics Application with a range of 200−700 nm at a scan rate of 4800 nm min^{-1} with two cycles (0.2 min delay between scans for 3 min, and 1.0 min delay between scans for 50 min). Apo-IsdC-N was denatured by adding sodium docecyl sulfate (SDS, 2% by m/v) and then boiling the protein for 30 min.

RESULTS

Species Identification with MCD Spectroscopy. MCD spectroscopy has been shown to be a powerful technique not only in ligand identification of the Isd heme-binding proteins but also for tracking heme transfer.[30,36,45,46] A solution of 6 μM holo-IsdA-N, 0.6 μM apo-IsdC-N, and 9 μM IsdE was studied with continuous scanning MCD spectroscopy, Figure 1. As shown previously, holo-IsdA-N exhibits a very different MCD spectral trace than holo-IsdE due to the presence of different axial amino acid-binding ligands of the ferric heme-iron (Tyr (IsdA-N) to His (IsdE)), causing the heme iron spin to change from high to low spin.[36,45,46] This is marked by a large increase in the B-band MCD signal intensity at both 408 (+) and 423 nm (−) in the MCD spectrum. The absolute value of the MCD signal intensity at 422 nm is shown in the inset of Figure 1. There is a steady increase in the MCD signal magnitude, indicating transfer of heme from IsdA-N to IsdE through IsdC-N. However, due to the substoichiometric amount of apo-IsdC-N present in solution and the significant overlap of the spectral envelops of holo-IsdA-N, IsdC-N, and holo-IsdE species in solution, it was not possible to track the concentration of holo-IsdC-N, and it was very difficult to quantify the time-dependent concentration of the holo-IsdA-N in solution by MCD spectroscopy. Therefore, in order to track all species in solution and create an accurate kinetic map of the reaction, ESI-MS was used to solve the problem.

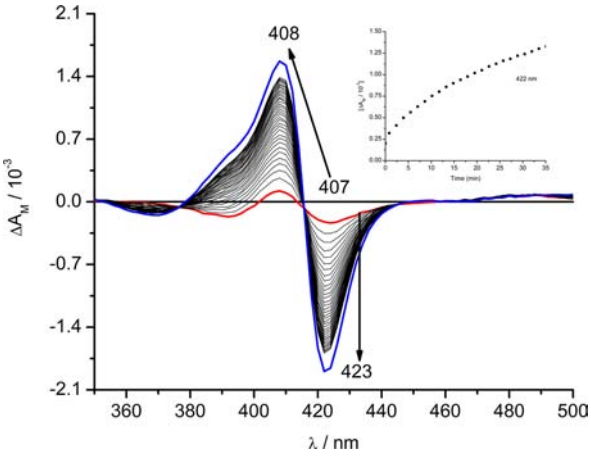

Figure 1. MCD spectra recorded during the reaction between holo-IsdA-N, a stoichiometrically limited amount of apo-IsdC-N, and apo-IsdE. Spectral changes are observed for the heme transfer from IsdA-N to IsdE through IsdC-N.

ESI-MS Data Show Real-Time Transfer of Heme from IsdA-N to IsdC-N and Then to IsdE. The ESI-MS technique is able to identify all of the six protein species involved in the heme-transfer reaction, which include heme-bound, holo-IsdA-N, holo-IsdC-N, and holo-IsdE. ESI-MS can also measure the spectroscopically silent apo-IsdA-N, apo-IsdC-N, and apo-IsdE. The mass spectral data were obtained from a single, mixed solution.

From previous work, it was shown that apo-IsdC-N efficiently removes heme from holo-IsdA-N and then transfers heme to apo-IsdE.[25,36] Apo-IsdE does not remove heme from holo-IsdA-N. Since each NEAT domain contains a distinct amino acid composition, and therefore, a distinct mass, a reaction similar to the MCD experiment was performed using time-resolved ESI-MS, Figure 2, with Isd species concentrations of 6 μM holo-IsdA-N, 0.45 μM holo-IsdC-N, and 12 μM IsdE. Since the first measured point was approximately 0.5 min, holo-IsdC-N was used instead of apo-IsdC-N to circumvent the first filling step of apo-IsdC-N, and therefore, the kinetic map is more accurate. With these concentrations, the stoichiometric ratio of IsdA-N:IsdC-N:IsdE was approximately 1:0.075:2, meaning that IsdC-N must turn over approximately 13 times to complete the reaction and transfer all heme to apo-IsdE, thereby imparting the role of heme shuttle onto IsdC-N.

The time-dependent charge state data reveal all six possible species in solution: IsdA-NEAT (AA), apo-IsdC-NEAT (AC), and apo-IsdE (AE) species and the heme-bound species holo-IsdA-NEAT (HA), holo-IsdC-NEAT (HC), and holo-IsdE (HE). In the ESI-MS data the +8 and +7 charge states were observed for IsdA-N, +9 and +8 for IsdC-N, and +13 to +11 for IsdE. Early in the reaction (0.5 min), the formation of holo-IsdE is detected, together with solely holo-IsdC-N (specifically no apo-IsdC-N was detected), indicating that the filling of IsdC-N from IsdA-N is faster than transfer to IsdE, resulting in a buildup of holo-IsdC-N.

Progressing through the reaction, the disappearance of charge states associated with holo-IsdA-N is observed coincident with the appearance of the apo-IsdA-N charge states. By the 10 min mark, only apo-IsdA-N charge states are observed, with no holo-IsdA-N charge states. After 20 min, the spectral data show the presence of a remaining but limited fraction of holo-IsdC-N and a large fraction of apo-IsdC-N, together with apo-IsdA-N. Interestingly, in the kinetic reactions we find that there is always a significant fraction of holo-IsdC-N detectable at the end of the reaction. This atypical result does not match previously recorded unidirectional heme transfer, which was found to leave the donor completely heme-free.[32] The IsdE is approximately 50% holo, which corresponds

dx.doi.org/10.1021/ja305115y | J. Am. Chem. Soc. 2012, 134, 16578−16585

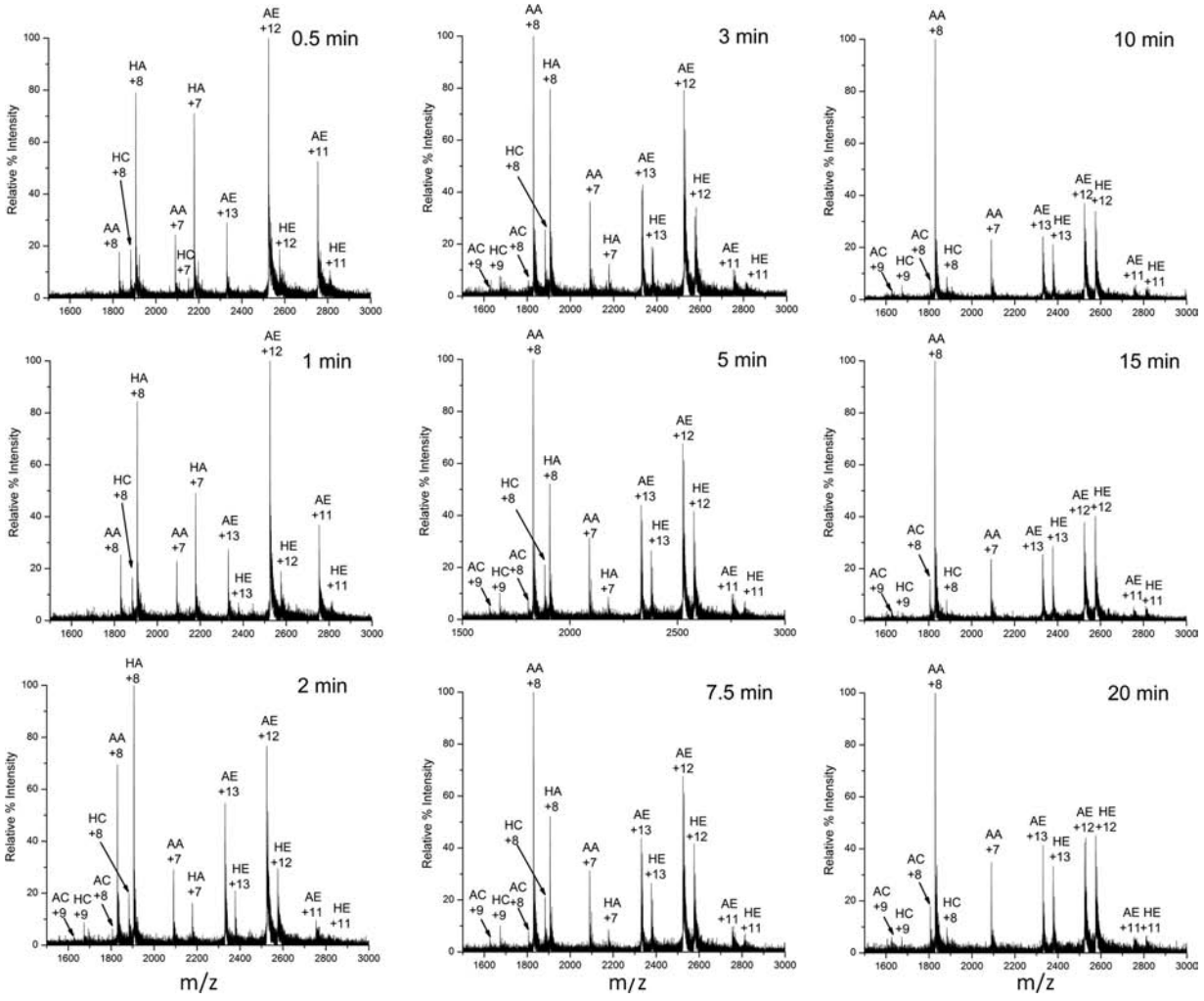

Figure 2. Mass spectral data recorded during heme transfer from IsdA-N to IsdE via IsdC-N. ESI-MS charge states are shown at nine time intervals (0.5, 1.0, 2.0, 3.0, 5.0, 7.5, 10, 15, and 20 min) for the heme-free apo-IsdA-NEAT (AA), apo-IsdC-NEAT (AC), and apo-IsdE (AE) species and the heme-bound holo-IsdA-NEAT (HA), holo-IsdC-NEAT (HC), and holo-IsdE (HE) species. +8 and +7 charge states were observed for IsdA-N, +9 and +8 for IsdC-N, and +13 to +11 for IsdE. At the start of the reaction the concentrations were as follow: HA, 6.0 μM; HC, 0.45 μM; and AE, 12 μM. The temperature was 15 °C.

stoichiometrically to the predicted stoichiometry of the reaction.

Determination of the Reaction Mechanism and the Rates of Reaction. To determine the mechanism of the reaction and the associated reaction rates, a multifunctional analysis[44] was carried out. Quantification of charge state data requires that both apo- and holo-Isd proteins have similar charge state distributions; therefore, by making apo and holo peaks relative to each other, it was possible to calculate concentrations.[36,40] For this analysis, all the data points were simultaneously fitted with a set of sequential bimolecular reaction equations. The changes in the concentration of each of the six species as a function of time are best seen in the summary plot, Figure 3.

The cog-wheel-like mechanism of heme transfer where IsdC-N acts as a heme shuttle is not a straightforward reaction. Fits with either a completely irreversible mechanism or a completely reversible mechanism did not fit the time-resolved data measured for the heme transfer for each protein (see Supporting Information). Scheme 1 provides an outstanding fit to the data (Figure 3) with a very straightforward mechanism.

The unexpected chemistry that results in some of the heme being essentially frozen in IsdC-N (reaction (3) in Scheme 1) must lie in the turnover of IsdC-N itself, that is, the filling of apo-IsdC-N from holo-IsdA-N and subsequent transfer to apo-IsdE. This is taken into account in Scheme 1, where the heme transfer from holo-IsdA-N to apo-IsdC-N results in apo-IsdA-N and holo-IsdC-N*. Holo-IsdC-N* is an inactive heme-transfer protein that is indistinguishable from native holo-IsdC-N. The time-dependent ESI-MS results from Figure 2 and the fits using Scheme 1 are shown in Figure 3. The rate constants are shown in Table 1. The rate constant for transfer from holo-IsdA-N to apo-IsdC-N (k_1) is approximately 2.5 times the rate constant for the transfer of heme from holo-IsdC-N to apo-IsdE (k_2). The reaction rate constant that disables IsdC-N is approximately 9 times slower than that for heme transfer from holo-IsdC-N to apo-IsdE, the slowest of the two heme transfers. Therefore, the progression to the disabled IsdC-N is slow but steady.

The reactions in Scheme 1 were tested by performing the same reaction as in Figure 2 but with an increase in holo-IsdC-N (Figure S2). At the start of the reaction the concentrations were HA = 6.0 μM, HC = 1.2 μM, and AE = 12 μM. By

dx.doi.org/10.1021/ja305115y | J. Am. Chem. Soc. 2012, 134, 16578−16585

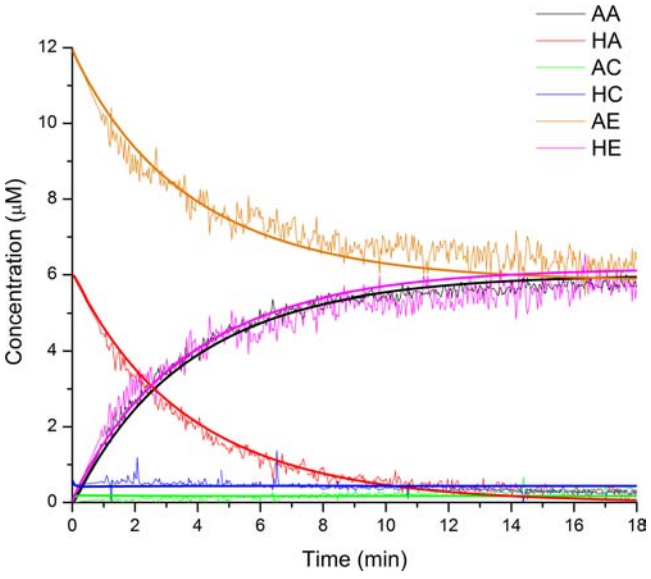

Figure 3. Fits to the experimental ESI-MS data using Scheme 1 with the data from Figure 2. The experimentally determined concentrations (apo-IsdE, yellow; holo-IsdE, purple; apo-IsdA-N, black; holo-IsdA-N, red; apo-IsdC-N, green; and holo-IsdC-N, blue) are superimposed by the smooth lines that represent the best fit to all the data based on Scheme 1. At the start of the reaction the concentrations were as follow: HA, 6.0 μM; HC, 0.45 μM; and AE, 12 μM. The temperature was 15 °C.

Scheme 1. Irreversible Reaction Mechanism Used To Fit the Experimental Data from Figure 2

$$\text{holo-IsdA-N + IsdC-N} \xrightarrow{k_1} \text{IsdA-N + holo-IsdC-N} \quad (1)$$

$$\text{holo-IsdC-N + IsdE} \xrightarrow{k_2} \text{IsdC-N + holo-IsdE} \quad (2)$$

$$\text{holo-IsdA-N + IsdC-N} \xrightarrow{k_3} \text{IsdA-N + holo-IsdC-N*} \quad (3)$$

Table 1. Bimolecular Rate Constants for Figure 2B: A Mechanism Based on Scheme 1

kinetic parameters using the Scheme 1 mechanism (second-order rate constants)	specific rate constant/μM^{-1} s^{-1}
k_1	$2.3 \times 10^{-2} \pm 0.2 \times 10^{-2}$
k_2	$9.6 \times 10^{-3} \pm 0.3 \times 10^{-3}$
k_3	$1.1 \times 10^{-3} \pm 0.1 \times 10^{-3}$

approximately doubling the amount of holo-IsdC, both parts of the reaction would be affected by a concentration change. This reaction was fitted with the kinetic parameters from Table 1. The fit confirms the results from Table 1. This model is an accurate and simple explanation of the kinetics observed when IsdC-N acts as a heme shuttle and turns over heme from IsdA-N to IsdE.

UV−Visible Absorption Data Indicate That Protein Confirmation Is Important for Heme Transfer. A control experiment was performed in order to test if only intact apo-IsdC-N can bind heme from holo-IsdA-N in order to transfer heme to apo-IsdE or if IsdC-N acts as an independent facilitator, whereby apo-IsdC-N acts as a trigger to facilitate heme transfer between holo-IsdA-N and apo-IsdE, Figure 4. Figure 4A shows that heme does not dissociate or transfer from holo-IsdA-N to IsdE within the time frame of the kinetic measurements. The Soret band for holo-IsdA-N and holo-IsdC-N is at 403 nm due to Tyr ligand binding, while it would shift to 413 nm for holo-IsdE due to His binding. However, this Soret band shift is immediately observed when apo-IsdC-N is added to a solution of holo-IsdA-N and apo-IsdE, Figure 4B, showing that heme transfer from holo-IsdA-N to apo-IsdE has occurred. This result was mirrored in Figure 1 with the time-dependent MCD results. In a further test, denatured apo-IsdC-N was added to a mixture of holo-IsdA-N and apo-IsdE to test if native IsdC-N is required for the heme-transfer reaction to take place, Figure 4C. The data show that no heme transfer

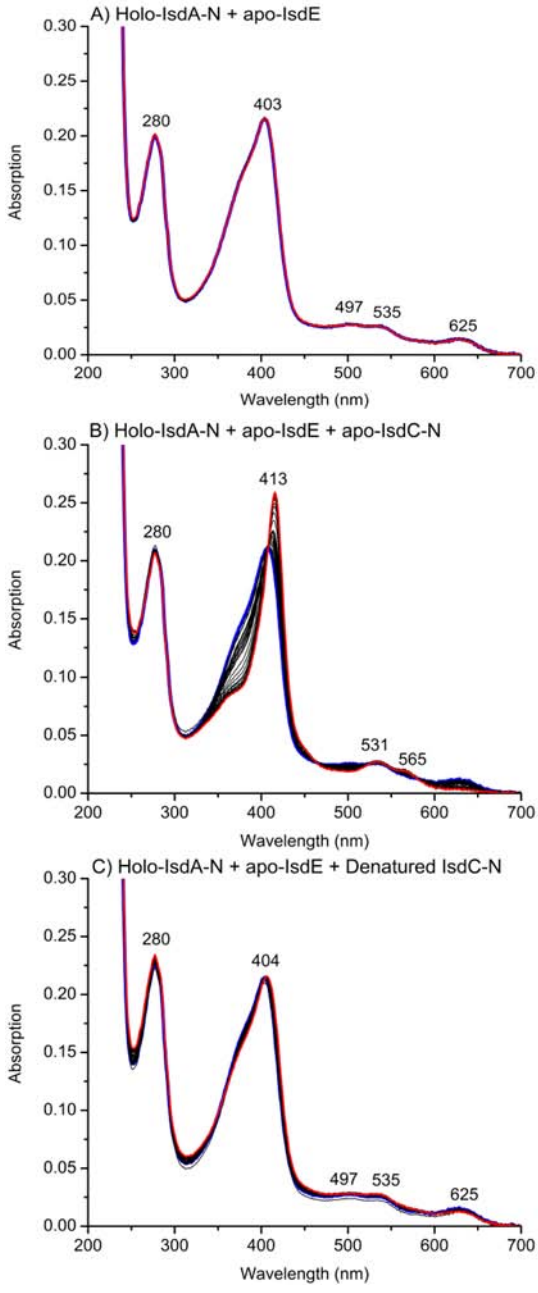

Figure 4. Heme-transfer reactions showing the importance of intact IsdC-N by UV−visible absorption spectroscopy: (A) 6.0 μM holo-IsdA-N with 12 μM apo-IsdE, showing lack of heme transfer; (B) 6.0 μM holo-IsdA-N, 0.6 μM apo-IsdC-N, and 12 μM apo-IsdE, showing heme transfer from IsdA-N→IsdC-N→IsdE; (C) 6.0 μM holo-IsdA-N, 0.6 μM denatured apo-IsdC-N, and 12 μM apo-IsdE, indicating no heme transfer. Each experiment was carried out for 30 min (within the experimental time frame of the other kinetic experiments presented).

dx.doi.org/10.1021/ja305115y | J. Am. Chem. Soc. 2012, 134, 16578−16585

from holo-IsdA-N occurred to apo-IsdE within the experimental time frame, although a slight wavelength change is detectable in the Soret band of the holo-IsdA-N. This could indicate slight interactions with SDS that was added to the solution when apo-IsdC-N was added. Nonetheless, no heme transfer was observed.

DISCUSSION

The proposed role of the Isd proteins is to shuttle heme through the cell wall and membrane of *S. aureus*. Two important questions arise: (i) What is the actual mechanism for the heme transfer following heme acquisition from hemoglobin or haptoglobin−hemoglobin? (ii) Can the Isd system act as a cog-wheel with respect to heme transfer, by which we mean, can the same Isd proteins keep transferring heme in sequence? With respect to question (i), previous equilibrium studies have shown that heme transfer takes place from holo-IsdA-N to apo-IsdC-N and also from holo-IsdC-N to apo-IsdE unidirectionally,[25,36] implying protein-to-protein transfer is involved rather than a dissociative reaction mechanism, which would not impose the specificity of the reaction observed. These weak protein−protein interactions have been shown where heme transfer resulted from a hand-clasp model between the alpha and beta loops in the Isd protein structure just outside of the heme pocket. These interactions facilitate the association of the NEAT domains of Isd-A and IsdC-N, forming an interactive complex.[35] Furthermore, it was determined that the heme-transfer rates from IsdA to IsdC and IsdC to IsdE were >70 000 times faster than simple heme dissociation due to protein−protein interactions.[31] The data presented in this work also show a requirement for protein−protein interactions rather than a series of coupled dissociative/associative reactions, and this is in agreement with the recent findings of others.[47]

Key to being able to answer question (ii) is the development of a technique that can differentiate between spectroscopically similar species and spectroscopically silent species regardless of the number of protein species in solution. Time-dependent ESI-MS data are able to perform this task. Quantitative analysis of charge state data can be performed since the apo and holo confirmation of the Isd proteins contain similar charge states. Hence, apo and holo charge states can be used relatively to each other to quantitate the Isd species measured be ESI-MS.[7,30,36,48,49] To answer question (ii), the complete system and the values of the rate constants reported here must be taken into account. IsdB and IsdH were proposed as the starting points of the heme transfer through the relatively thick (ca. 90 nm) peptidoglycan cell wall, with transfer via IsdA to IsdC and then on to IsdE. It is reasonable to assume that IsdE, which is located at the membrane surface, serves as the acceptor for heme prior to its passage through the membrane and into the cytoplasm, where heme is then met by the heme-degrading enzymes IsdG and IsdI.[18−20]

Relative Rates of Heme Transfer between Isd Species. The values of the specific rate constants for heme transfer from Table 1 for the model that fits the reaction mechanism in Scheme 1 are 2.3×10^{-2} μM^{-1} s^{-1} for the first step from holo-IsdA-N to apo-IsdC-N (k_1) and 9.6×10^{-3} μM^{-1} s^{-1} for the second step from holo-IsdC-N to IsdE (k_2). The reaction rates are different by a factor of ~2.5 (k_1/k_2). Since NEAT-to-NEAT heme transfer is relatively fast,[25] this difference between the first step and the second step has a major ramification: heme will rapidly build-up in IsdC in the cell wall before slowly transferring to IsdE, the protein located on the membrane as part of the ABC transporter.

Overall, these results may explain the importance of a multistep heme-transfer mechanism. The introduction of the requirement for the intervention of a single protein in the heme-transfer mechanism is restrictive. The data presented here, and specifically the disparity in transfer rates, suggest a possible explanation: if heme transfer was slow from IsdA to IsdC, then free heme exposed during the extraction from hemoglobin, which involves IsdH and IsdB, might be lost to the bacterium. With a fast heme-transfer rate into a wall-bound protein (IsdC), heme is moved deeper into the cell wall of the bacterium, where it is more protected from the extracellular milieu. The subsequent slower heme transfer from IsdC to IsdE can act as a throttle for the system to control the eventual heme transport into and buildup in the cytoplasm; indeed, Skaar and co-workers have demonstrated heme toxicity in *S. aureus*.[50]

The Disabling Step of IsdC-N Is Slow. This slow progressive step, ~9 times slower than normal transfer from IsdC-N to IsdE, affects the overall kinetic model and the heme-transfer kinetic results. Key to the reaction is the treatment of IsdC-N. The limited concentration of IsdC-N imparts a critical role on this protein so that IsdC-N acts a central cog-wheel in the heme-transfer system. IsdC-N plays the role of shuttling heme from IsdA-N to IsdE, where IsdC-N would need to turnover approximately 10 times before the reaction is finished under the experimental conditions used in this work. Although the disabling step may exist for all Isd proteins when cycling heme, the disabling step may be due to the proteins not being compartmentalized in the cell wall. Further research is needed to look at the wall-anchored protein−protein interactions to further investigate this disabling step.

Intact Isd Proteins Are Required To Transfer Heme. The mass spectral data in Figure 2 provide one more important piece of information about the reaction. Charge states in the ESI mass spectrum are sensitive to changes in the volume of the protein and, therefore, provide a measure of changes in solvent access to the protein's basic amino acid residues. Protein integrity during the heme-transfer reaction can be determined directly from the charge state distribution.[29,30,36,45,46] The data show that no major changes in the charge state distribution occur for the apo and holo species of IsdA-N, IsdC-N, and IsdE. This indicates that no significant structural changes took place as a result of heme binding or release in any of these proteins. No protein degradation was observed; this observation was particularly important with respect to IsdC-N following its turnovers.

The UV−visible absorption experiments show how important IsdC-N is to protein−protein interactions with regard to heme transfer. Significantly, disruption of the hand-clasp model by protein denaturation completely disables heme transfer.[35]

CONCLUSIONS

Overall, the model proposed in this study treats IsdC-N as a central cog-wheel in the important through-cell-wall heme-transfer pathway of the Isd system (IsdA-N, IsdC-N, and IsdE). The model suggests that intact substoichiometic amounts of IsdC-N are crucial to heme transfer from IsdA-N to IsdE because heme does not transfer from IsdA-N directly to IsdE. Overall, the rate of transfer from IsdA-N to IsdC-N is faster than transfer from IsdC-N to IsdE, which may impart heme cytotoxicity relief for the bacterium by throttling the heme-

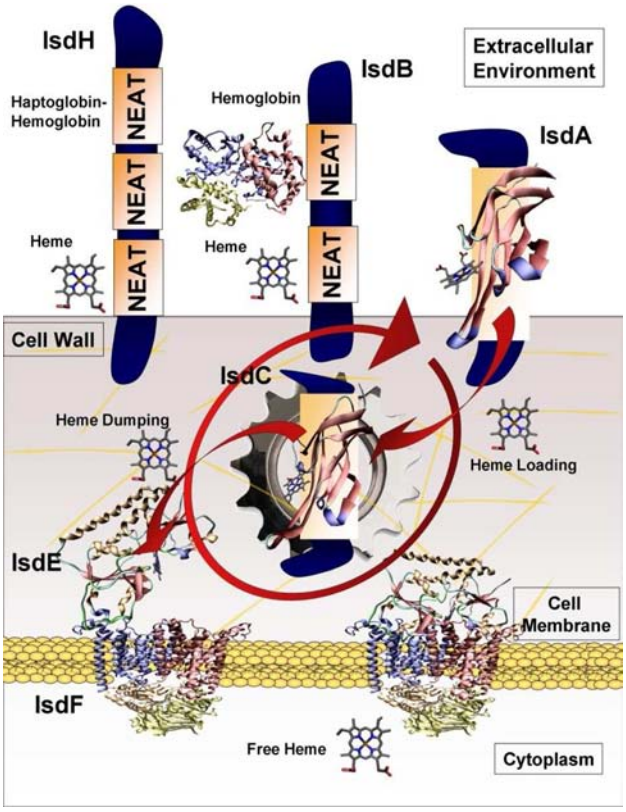

Figure 5. Heme transport model based on analysis of the mass spectral data obtained from this study. Unidirectional heme transfer takes place from IsdA-N to IsdC-N to IsdE, and the diagram indicates that IsdC-N cycles round, acting as a cog-wheel in the overall transfer reaction. There is no direct transfer from holo-IsdA-NEAT to apo-IsdE. The mass spectral data to support the model are in agreement with the model first proposed by Schneewind and colleagues.[17]

transfer reaction into the cell interior. Key to the transfer reaction mechanism used to account for the experimental data is the disabling of IsdC-N, which also may be important for heme toxicity protection. Figure 5 summarizes the results found in this research. The conclusions are (i) that IsdC (here studied as IsdC-N) is the central cog-wheel in heme transfer through the *S. aureus* wall and acts as a courier between IsdA and IsdE by cycling between IsdC and IsdE multiple times and (ii) that the differential in rates supports a hypothesis that heme stockpiling in the wall may take place as a result of efficient scavenging but more restricted influx via the membrane transporters reduces possible subsequent heme toxicity.

■ ASSOCIATED CONTENT

Supporting Information

Other general fits (irreversible and reversible) that do not fit the data presented and another trial run to support the data presented in this paper. This material is available free of charge via the Internet at http://pubs.acs.org.

■ AUTHOR INFORMATION

Corresponding Author

martin.stillman@uwo.ca

Notes

The authors declare no competing financial interest.

■ ACKNOWLEDGMENTS

This work was supported by operating and equipment grants from the Natural Sciences and Engineering Research Council (NSERC) of Canada (to M.J.S.), the Canadian Institutes of Health Research (to D.E.H.), the Ontario Graduate Scholarship in Science and Technology program, and an NSERC Canada Graduate Scholarship (to M.T.T.).

■ REFERENCES

(1) Papanikolaou, G.; Pantopoulos, K. *Toxicol. Appl. Pharmacol.* **2005**, *202*, 199−211.
(2) Bullen, J. J.; Rogers, H. J.; Griffiths, E. *Curr. Top. Microbiol. Immun.* **1978**, *80*, 1−35.
(3) Genco, C. A.; Dixon, D. W. *Mol. Microbiol.* **2001**, *39*, 215−220.
(4) Skaar, E. P.; Schneewind, O. *Microbes Infect.* **2004**, *6*, 390−397.
(5) Wandersman, C.; Delepelaire, P. *Annu. Rev. Microbiol.* **2004**, *58*, 611−647.
(6) Wandersman, C.; Stojiljkovic, I. *Curr. Opin. Microbiol.* **2000**, *3*, 390−397.
(7) Grigg, J. C.; Mao, C. X.; Murphy, M. E. P. *J. Mol. Biol.* **2011**, *413*, 684−698.
(8) Tiedemann, M. T.; Muryoi, N.; Heinrichs, D. E.; Stillman, M. J. *Biochem. Soc. Trans.* **2008**, *36*, 1138−1143.
(9) Tong, Y.; Guo, M. *Arch. Biochem. Biophys.* **2009**, *481*, 1−15.
(10) Gordon, R. J.; Lowy, F. *Clin. Infect. Dis.* **2008**, *46*, S350−359.
(11) McGowan, J. E.; Tenover, F. C. *Nature Rev.* **2004**, *2*, 251−259.
(12) Pilpa, R. M.; Robson, S. A.; Villareal, V. A.; Wong, M. L.; Phillips, M.; Clubb, R. T. *J. Biol. Chem.* **2009**, *284*, 1166−1176.
(13) Torres, V. J.; Pishchany, G.; Humayun, M.; Schneewind, O.; Skaar, E. P. *J. Bacteriol.* **2006**, *188*, 8421−8429.
(14) Mazmanian, S. K.; Ton-That, H.; Su, K.; Schneewind, O. *Proc. Natl. Acad. Sci. U.S.A.* **2002**, *99*, 2293−2298.
(15) Morrissey, J. A.; Cockayne, A.; Hammacott, J.; Bishop, K.; Denman-Johnson, A.; Hill, P. J.; Williams, P. *Infect. Immun.* **2002**, *70*, 2399−2298.
(16) Taylor, J. M.; Heinrichs, D. E. *Mol. Microbiol.* **2002**, *43*, 1603−1614.
(17) Mazmanian, S. K.; Skaar, E. P.; Gaspar, A. H.; Humayun, M.; Gornicki, P.; Jelenska, J.; Joachmiak, A.; Missiakas, D. M.; Schneewind, O. *Science* **2003**, *299*, 906−909.
(18) Skaar, E. P.; Gaspar, A. H.; Schneewind, O. *J. Biol. Chem.* **2004**, *279*, 436−443.
(19) Lee, W. C.; Reniere, M. L.; Skaar, E. P.; Murphy, M. E. *J. Biol. Chem.* **2008**, *283*, 30957−30963.
(20) Reniere, M. L.; Ukpabi, G. N.; Harry, S. R.; Stec, D. F.; Krull, R.; Wright, D. W.; Bachmann, B. O.; Murphy, M. E.; Skaar, E. P. *Mol. Microbiol.* **2010**, *75*, 1529−1538.
(21) Corrigan, R. M.; Miajlovic, H.; Foster, T. J. *BMC Microbiol.* **2009**, 9.
(22) Clarke, S. R.; Wiltshire, M. D.; Foster, S. J. *Mol. Microbiol.* **2004**, *51*, 1509−1519.
(23) Palazzolo, A. M.; Reniere, M. L.; Braughton, K. R.; Sturdevant, D. E.; Otto, M.; Kreiswirth, B. N.; Skaar, E. P.; DeLeo, F. R. *J. Immunol.* **2008**, *180*, 500−509.
(24) Cheng, A. G.; Kim, H. K.; Burts, M. L.; Krausz, T.; Schneewind, O.; Missiakas, D. M. *FASEB J.* **2009**, *23*, 3393−3404.
(25) Zhu, H.; Xie, G.; Liu, M.; Olson, J.; Fabian, M.; Dooley, D.; Lei, B. *J. Biol. Chem.* **2008**, *283*, 18450−18460.
(26) Dryla, A.; Gelbmann, D.; Gabain, A. v.; Nagy, E. *Mol. Microbiol.* **2003**, *49*, 37−53.
(27) Watanabe, M.; Tanaka, Y.; Suenaga, A.; Kurodo, M.; Yao, M.; Watanabe, N.; Arisaka, F.; Ohta, T.; Tanaka, I.; Tsumoto, K. *J. Biol. Chem.* **2008**, *283*, 28649−28659.
(28) Mack, J.; Vermeiren, C.; Heinrichs, D. E.; Stillman, M. J. *Biochem. Biophys. Res. Commun.* **2004**, *320*, 781−788.
(29) Pluym, M.; Vermeiren, C. L.; Mack, J.; Heinrichs, D. E.; Stillman, M. J. *J. Porphyrins Phthalocyanines* **2007**, *11*, 165−171.

(30) Tiedemann, M. T.; Muryoi, N.; Heinrichs, D. E.; Stillman, M. J. *J. Porphyrins Phthalocyanines* **2009**, *13*, 1006−1016.
(31) Liu, M.; Tanaka, W. N.; Zhu, H.; Xie, G.; Dooley, D. M.; Lei, B. *J. Biol. Chem.* **2008**, *283*, 6668−6678.
(32) Grigg, J. C.; Vermeiren, C. L.; Heinrichs, D. E.; Murphy, M. E. *Mol. Microbiol.* **2007**, *63*, 139−149.
(33) Sharp, K. H.; Schneider, S.; Cockayne, A.; Paoli, M. *J. Biol. Chem.* **2007**, *282*, 10625−10631.
(34) Grigg, J. C.; Vermeiren, C. L.; Heinrichs, D. E.; Murphy, M. E. *J. Biol. Chem.* **2007**, *282*, 28815−28822.
(35) Villareal, V. A.; Spirig, T.; Robson, S. A.; Liu, M.; Lei, B.; Clubb, R. T. *J. Am. Chem. Soc.* **2011**, *133*, 1417−14179.
(36) Muryoi, N.; Tiedemann, M. T.; Pluym, M.; Cheung, J.; Heinrichs, D. E.; Stillman, M. J. *J. Biol. Chem.* **2008**, *283*, 28125−28136.
(37) Boys, B. L.; Konermann, L. *J. Am. Soc. Mass. Spectrom.* **2006**, *18*, 8−16.
(38) Hathout, Y.; Fabris, D.; Fenselau, C. *Int. J. Mass Spectrom.* **2001**, *204*, 1−6.
(39) Konermann, L.; Collings, B. A.; Douglas, D. J. *Biochemistry* **1997**, *36*, 5554−5559.
(40) Ngu, T.; Lee, J.; Rushton, M. K.; Stillman, M. J. *Biochemistry* **2009**, *38*, 8806−8816.
(41) Zaia, J.; Fabris, D.; Wei, D.; Karpel, R. L.; Fenselau, C. *Protein Sci.* **1998**, *7*, 2398−2404.
(42) Guzman, L.-M.; Belin, D.; Carson, M. J.; Beckwith, J. *J. Bacteriol.* **1995**, *177*, 4121−4130.
(43) Li, J. M.; Umanoff, H.; Proenca, R.; Russell, C. S.; Cosloy, S. D. *J. Bacteriol.* **1988**, *170*, 1021−1025.
(44) Hoops, S.; Sahle, S.; Gauges, R.; Lee, C.; Pahle, J.; Simus, N.; Singhal, M.; Xu, L.; Mendes, P.; Kummer, U. *Bioinformatics* **2006**, *22*, 3067−3074.
(45) Pluym, M.; Muryoi, N.; Heinrichs, D. E.; Stillman, M. J. *J. Inorg. Biochem.* **2008**, *102*, 480−488.
(46) Pluym, M.; Vermeiren, C. L.; Mack, J.; Heinrichs, D. E.; Stillman, M. J. *Biochemistry* **2007**, *46*, 12777−12787.
(47) Abe, R.; Caaveiro, J. M. M.; Kozuka-Hata, H.; Oyama, M.; Tsumoto, K. *J. Biol. Chem.* **2012**, *287*, 16477−16487.
(48) Kaltashov, I. A.; Fabris, D.; Fenselau, C. C. *J. Phys. Chem.* **1995**, *99*, 10046−10051.
(49) Grigg, J. C.; Ukpabi, G.; Gaudin, C. F. M.; Murphy, M. E. P. *J. Inorg. Biochem.* **2010**, *104*, 341−348.
(50) Torres, V. J.; Stauff, D. L.; Pishchany, G.; Bezbradica, J. S.; Gordy, L. E.; Iturregui, J.; Anderson, K. L.; Dunman, P. M.; Joyce, S.; Skaar, E. P. *Cell Host Microbe* **2007**, *1*, 85−87.